論文 / 著書情報
Article / Book Information

Title	Difference-Beam Operation in a Center-Fed Dual-Polarized Parallel-Plate Waveguide Slot Array Antenna
Authors	Huanqian Xiong, Jiro Hirokawa, Takashi Tomura
Citation	IEICE Communications Express, Vol. 13, Issue 9, pp. 359-362
Pub. date	2024, 7
DOI	https://dx.doi.org/10.23919/comex.2024XBL0100
Creative Commons	Information is in the article.
権利情報 / Copyright	本著作物の著作権は電子情報通信学会に帰属します。 Copyright(c) 2024 IEICE

IEICE Communications Express, Vol.13, No.9, 359–362

ComEX

LETTER

Difference-beam operation in a center-fed dual-polarized parallel-plate waveguide slot array antenna

Huanqian Xiong[1, a)], **Jiro Hirokawa**[1], **and Takashi Tomura**[1]

Abstract This letter deals with the difference-beam operation in a center-feed dual-polarized parallel-plate waveguide slot array antenna at 24.5GHz, which consists of two orthogonally arranged 20×19 arrays of radiating slot pairs. A center-feeding scheme is employed in this design. Each rectangular feeding waveguide, fed by a probe, can feed half of the radiating panel, enabling easy control of the phase difference. Experimental results show that the monopulse antenna array has a bandwidth of 12.8% for reflections below −10 dB while it produces the sum beams, and 13.3% to produce the difference beams. Port isolation between the sum mode and difference mode is above 15 dB within the working frequency band. The measured realized gain of the sum beam is 31.3 dBi at 24.5 GHz, and the measured null-depth is below −33.9 dB for both polarizations.

Keywords: dual polarized antenna, monopulse antenna, parallel-plate waveguide antenna, slot array antenna
Classification: Antennas and propagation

1. Introduction

Monopulse array antennas, which produce sum and difference beams, have been widely used in radar systems for target tracking as they can provide accurate directional information [1].

One common variant is the microstrip monopulse array antenna, which employs a microstrip-line comparator and a radiating array [2, 3], featuring a planar structure. Reflector antennas are also widely studied in this field. Though they are bulkier than the microstrip monopulse array antennas, a complex comparator network is not needed [4].

Planar waveguide monopulse array antennas are studied in order to obtain an improved antenna efficiency in a simpler planar structure. Research on monopulse planar waveguide array antennas mostly focuses on antennas with a corporate waveguide feeding network, where techniques such as post-wall waveguides [5, 6] or gap waveguides [7] are introduced. By separating the radiating part into subarrays, controlling the phase difference becomes more convenient in a corporate-fed antenna. However, extra layers of the monopulse comparator network are needed in the corporate-fed waveguide array antennas, increasing the cross-section of the antenna structure. In addition, realizing a dual-polarized monopulse antenna using a corporate waveguide feeding network is challenging as it may introduce a more complex and bulkier feeding structure. In [8], two identical corporate-fed monopulse planar waveguide antenna arrays are placed side by side to realize a dual-polarized antenna.

On the other hand, parallel plate waveguide slot array antennas typically include a single-layer radiating panel and a planar series feeding network [9, 10]. The PPW slot array antennas have a simpler structure and lower cross-sections than the corporate-fed planar waveguide array antennas. However, it is difficult to control the phase difference between the different parts of the radiating panel since they are not decoupled as in the corporate-fed waveguide array antennas. In the previous study [11], a dual-polarized PPW slot array antenna utilizing two rectangular feeding waveguides beneath the radiating panel was proposed. The feed waveguide of each polarization has to be divided into two parts for the center feed structure of the dual polarized PPW slot array, which is not needed in a single polarized one [9].

The novelty of this letter is to deal with the difference-beam operation while [11] dealt with the detailed antenna design and the sum-beam operation. By using four feeding points at the center of the antenna, we can directly connect a monopulse comparator to the antenna panel. For each polarization, since one feeding waveguide is split into two, the feeding phase of each half of the antenna array can be controlled independently. The antenna's operation is verified by simulated and measured results where the proposed antenna can produce both sum and difference beams without increasing the structural complexity.

2. Configuration of the array antenna

The dual-polarized parallel plate waveguide slot array antenna developed in [11] consists of a radiating panel and four WR-42 feeding waveguides drawn in red beneath it, as shown in Fig. 1 (a). In the radiating part, two identical 20 × 19 arrays of radiating slot pairs are positioned orthogonally. Radiating slots in each slot pair are placed collinearly to realize dual-polarization, instead of the offset slot pairs in a conventional parallel plate waveguide slot array antenna [9].

The feeding waveguides incorporate centrally positioned longitudinal feeding slots proposed in [10], which have been verified to enhance radiation performance and broaden the reflection bandwidth of the PPW slot array antenna. Each feeding slot needs to be paired with two inductive walls to realize the desired coupling between the TE_{10} wave inside the feeding waveguides and the desired quasi-TEM wave

[1] Dept. of Electrical Engineering, Tokyo Institute of Technology, Meguro-ku, Tokyo 152–8552, Japan
[a)] xiong.h.aa@m.titech.ac.jp

DOI: 10.23919/comex.2024XBL0100
Received May 22, 2024
Accepted June 3, 2024
Publicized July 9, 2024
Copyedited September 1, 2024

inside the PPW. Each waveguide is fed by a waveguide probe placed at the center part of the array antenna, which allows the control of the phase of each feeding waveguide.

The antenna is designed to operate at 24.5 GHz. The antenna frame including all four feeding waveguides are milled from a 5052 aluminium alloy block. The size of the parallel plate waveguide measures 213 mm × 213 mm. The PPW is filled with a 5 mm-thick expanded dielectric substrate (ϵ_r = 1.12), which is covered by a 0.2 mm-thick copper top plate.

3. Monopulse comparator

A 90° hybrid coupler (Pasternack PE2CP1150) with two coaxial cables is used as the monopulse comparator in the proposed antenna, as shown in Fig. 1 (b), where two coaxial cables have different lengths to compensate for the phase balance between two output ports of the monopulse comparator. When the IN1 port of the hybrid coupler is excited, a phase difference of 4.23° can be measured at 24.5 GHz from the two output ports. When the IN2 port of the hybrid coupler is excited, a phase difference of −169.30° can be measured at 24.5 GHz from the two output ports, as shown in Fig. 2. When Port 1 and Port 2 are excited, the antenna is y-polarized, and the antenna array produces the *XOZ* plane difference beam. When Port 3 and Port 4 are excited, the antenna is x-polarized, and the antenna array produces the *YOZ* plane difference beam. All working scenarios of the proposed antenna array are detailed in Table I.

When the antenna is y-polarized and produces the difference beam, the simulated aperture field distributions of amplitude and phase are illustrated in Fig. 3. The phase difference between Port 1 and Port 2 of the array antenna is set to 180° to simulate the antenna producing the difference beam. It can be observed from Fig. 3 (a) that the field is cancelled along the y-axis at the center while producing the difference beam. The simulated amplitude distribution of E_y for the sum beam is similar to that of the difference beam except that the field is not cancelled at the center. Figure 3 (b) shows that when the antenna produces the difference beam, the −x half and the +x half of the radiating panel has a phase difference around 180°, while the antenna producing

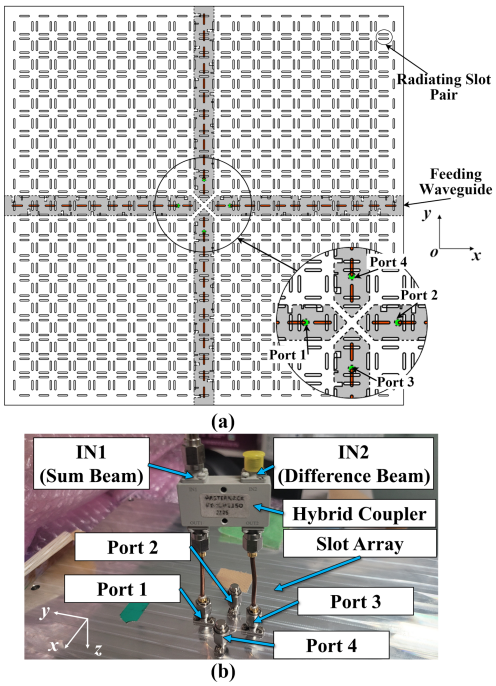

Fig. 1 (a) Top view of the dual-polarized parallel plate waveguide slot array antenna. (b) Monopulse comparator.

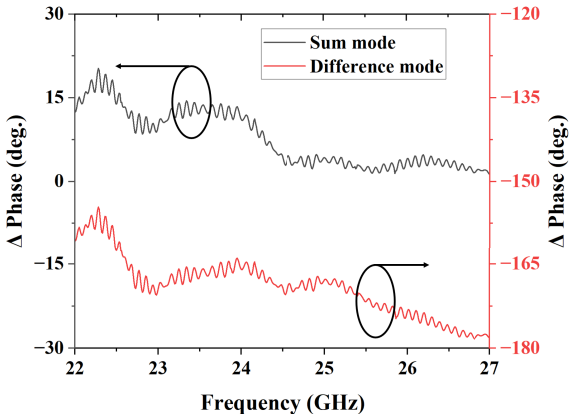

Fig. 2 Measured phase characteristics of the monopulse comparator.

Table I Realization of the dual-polarization and monopulse.

Mode	Array Port	Coupler Port	Polarization	Type
Mode1	1&2	IN1	Y-pol	$\Sigma_{\text{Y-pol}}$
Mode2	1&2	IN2	Y-pol	Δ_{El}
Mode3	3&3	IN1	X-pol	$\Sigma_{\text{X-pol}}$
Mode4	3&4	IN2	X-pol	Δ_{Az}

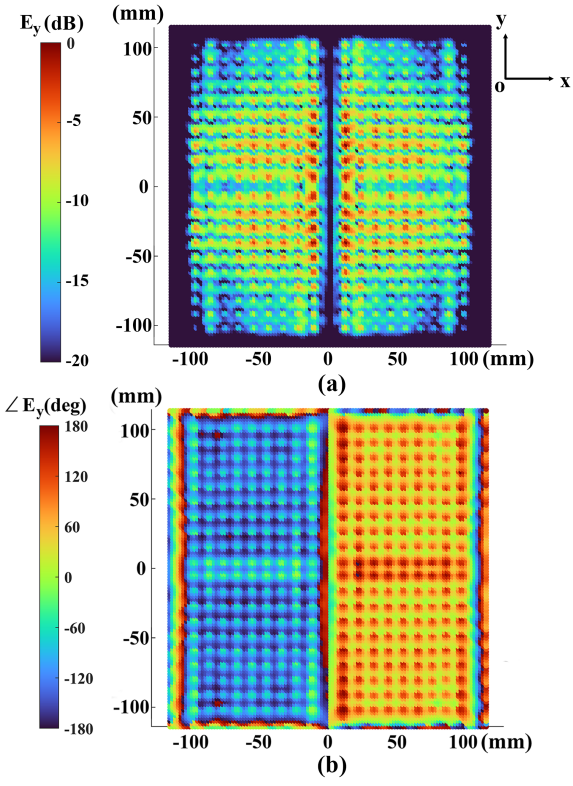

Fig. 3 (a) Simulated difference beam amplitude distribution of E_y at 24.5 GHz. (b) Simulated difference beam phase distribution of E_y at 24.5 GHz.

the sum beam has a uniform phase distribution.

4. Experimental results

4.1 S parameters

Figure 4 shows the reflection coefficients and the isolations of the monopulse antenna array measured by a vector network analyzer through the two input ports on the comparator. The bandwidth for the $\Sigma_{\text{Y-pol}}$ and $\Sigma_{\text{X-pol}}$ modes is 12.8% (23.38 - 26.58 GHz) and 12.9% (23.38 - 26.61 GHz) with the reflection below −10 dB. The reflection bandwidth for Δ_{El} and Δ_{Az} is 13.3% (23.41 - 26.76 GHz). The isolation is measured between the sum mode and difference mode that has the same polarization characteristics. The isolation is above 15 dB within the working frequency, which is limited by the isolation between the IN1 and IN2 ports of the Pasternack PE2CP1150 hybrid coupler.

4.2 Discussion on isolation

To enhance isolation between the sum and difference modes, several factors were investigated. Initially, $S_{(IN2,IN1)}$ of Pasternack PE2CP1150 hybrid coupler is around −15 dB, potentially constraining the monopulse antenna's isolation. Figure 5 illustrates the isolation variation with alternative

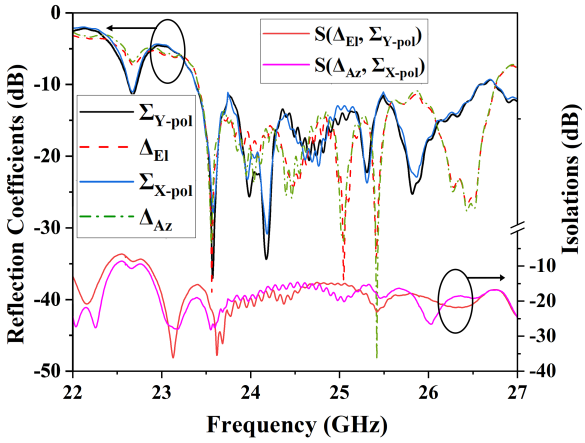

Fig. 4 Measured reflection coefficients and isolations of the monopulse antenna.

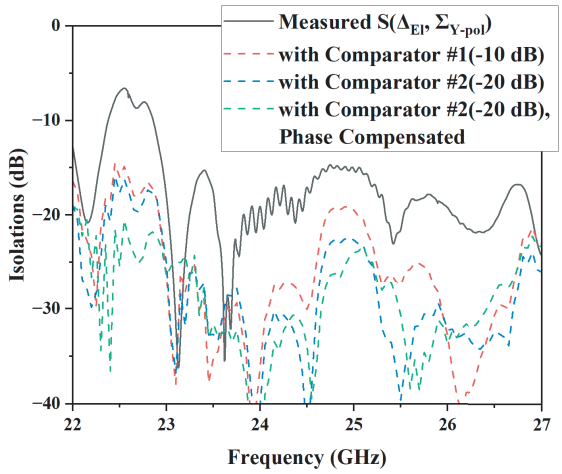

Fig. 5 Influence of the comparator performance on the isolation between the sum and difference mode.

comparators, computed using the slot array's measured S-parameters and two virtual comparators with $S_{(IN2,IN1)}$ reduced by 10 dB and 20 dB. Results indicate that a 20 dB enhancement in comparator isolation increases the isolation between modes of the monopulse antenna to over 22 dB.

Additionally, incomplete cancellation of reflections from the slot array can also increase coupling between modes. Fabrication tolerances causing port differences in slot array and comparator phase shifts depicted in Fig. 2 both contribute to this effect. While adjusting the monopulse comparator's phase difference to 0° and 180° marginally improves isolation, fabrication tolerances in the slot array remain limiting factors.

4.3 Radiation characteristics

The simulation model used for reference in this section has been adjusted according to the study in [11] due to fabrication tolerances and the inaccurate relative permittivity of the substrate inside the PPW. The relative permittivity in the adjusted model is set to 1.07 and a 0.2 mm-thick air gap is added between the substrate and the top plate of the PPW.

The measured realized gain of the sum beams is 31.3 dBi for both polarizations at 24.5 GHz with an antenna efficiency of 35.3%, as shown in Fig. 6. The simulated realized gain of the difference beams is 30.0 dBi at 24.5 GHz. The measured realized gains of the Δ_{El} and Δ_{Az} beams at 24.5 GHz are 29.8 dBi and 30.0 dBi, respectively.

At 24.5 GHz, the measured cross-polarization discrimination of the sum beams for both polarizations is above 26 dB, and the measured E-plane radiation patterns of the sum beams are in good agreement with the simulated results of the adjusted simulation model, as shown in Fig. 7. The H-plane radiation patterns of the sum beams are similar to those in the E-plane at 24.5 GHz except that the sidelobes around the end-fire directions are suppressed by the element pattern.

As shown in Fig. 8, the simulated null-depth of the difference beam is down to −46.6 dB. The measured null-depth of the Δ_{El} mode is −33.9 dB, and that of the Δ_{Az} mode is −47.7 dB at 24.5 GHz. The difference between the measured results of the two difference beams may be attributed to fabrication tolerances. The precision of the measurement

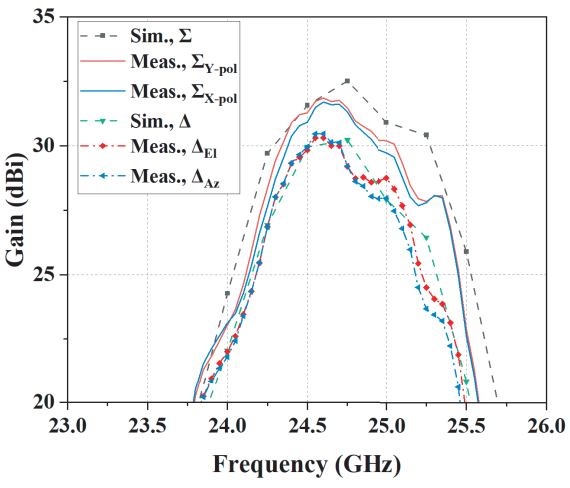

Fig. 6 Simulated and measured gains of the proposed antenna array.

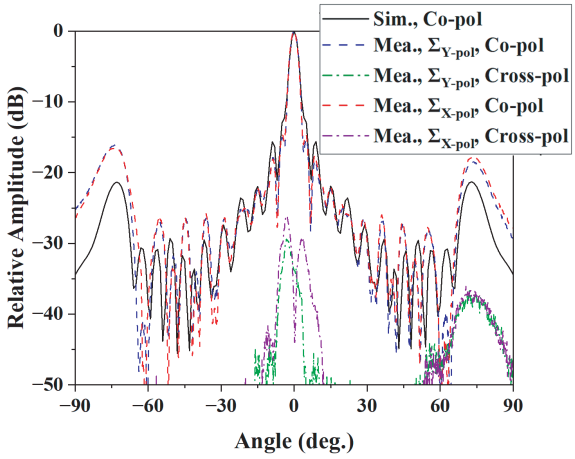

Fig. 7 Simulated and measured E-plane radiation patterns of the sum beams at 24.5 GHz.

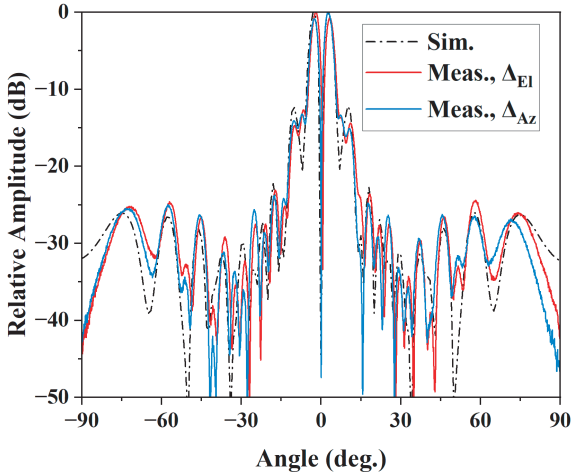

Fig. 8 Simulated and measured radiation patterns of the difference beams at 24.5 GHz.

Table II Performance comparison.

REF.	Freq. (GHz)	Null-Depth (dB)
[2]	14.25	−30
[4]	35	−30
[5]	10.3	−33.8
[7]	95	−35
[8]	15	−36
This work	24.5	−33.9(Δ_{El})/−47.7(Δ_{Az})

system's search capabilities can also contribute to the difference between the simulated and measured null depths. In general, the results show that the measured radiation patterns of the difference beams are in a good agreement with the simulated results. In comparison with previous works, a deeper null-depth of −47.7 dB is measured when the antenna produces Δ_{Az} mode, as shown in Table II.

5. Conclusions

In this letter, a dual-polarized monopulse PPW slot array antenna with a simple structure is proposed. The PPW slot array part is designed using a single-layer PPW radiating panel and four feeding waveguides beneath the panel with a operating frequency at 24.5 GHz. A CNC milled aluminum alloy block and etched copper plates are used to fabricate the prototype antenna. The proposed antenna features centered feeding probes, which enables the implementation of a simple monopulse comparator using a 90° hybrid coupler and two coaxial cables with a 90° phase difference. The measured reflection bandwidth of two difference modes reaches 13.3%, and that of the sum modes is 12.8% for y-polarization and 12.9% for x-polarization, with the reflection below −10 dB. The measured isolation between the sum and difference mode is over 15 dB, with additional solutions discussed for its further improvement. The measured realized gain of the sum beams at 24.5 GHz is 31.3 dBi for both polarizations. The measured null-depth at 24.5 GHz is −33.9 dB and −47.7 dB for elevation and azimuth plane difference beams. In general, the measured results show a good agreement with the simulated results, which verifies the soundness of the proposed antenna.

References

[1] S.M. Sherman and D.K. Barton, *Monopulse Principles and Techniques*., Artech, Norwood, 2011.

[2] H. Wang, D.-G. Fang, and X.G. Chen, "A compact single layer monopulse microstrip antenna array," *IEEE Trans. Antennas Propag.*, vol. 54, no. 2, pp. 503–509, Feb. 2006. DOI: 10.1109/TAP.2005.863103

[3] Y. Gao, W. Jiang, W. Hu, Q. Wang, W. Zhang and S. Gong, "A dual-polarized 2-D monopulse antenna array for conical conformal applications," *IEEE Trans. Antennas Propag.*, vol. 69, no. 9, pp. 5479–5488, Sept. 2021. DOI: 10.1109/TAP.2021.3060085

[4] J. Zhao, H. Li, X. Yang, W. Mao, B. Hu, T. Li, H. Wang, Y. Zhou, and Q. Liu, "A compact Ka-band monopulse Cassegrain antenna based on reflectarray elements," *IEEE Antennas Wireless Propag. Lett.*, vol. 17, no. 2, pp. 193–196, Feb. 2018. DOI: 10.1109/LAWP.2017.2779789

[5] W. Li, S. Liu, J. Deng, Z. Hu, and Z. Zhou, "A compact SIW monopulse antenna array based on microstrip feed," *IEEE Antennas Wireless Propag. Lett.*, vol. 20, no. 1, pp. 93–97, Jan. 2021. DOI: 10.1109/LAWP.2020.3041485

[6] Z. Wang, Y. Hu, L. Xiang, J. Xu, and W. Hong, "A wideband high-gain planar monopulse array antenna for Ka-band radar applications," *IEEE Trans. Antennas Propag.*, vol. 71, no. 11, pp. 8739–8752, Nov. 2023. DOI: 10.1109/TAP.2023.3312971

[7] A. Vosoogh, A. Haddadi, A.U. Zaman, J. Yang, H. Zirath, and A.A. Kishk, "W-band low-profile monopulse slot array antenna based on gap waveguide corporate-feed network," *IEEE Trans. Antennas Propag.*, vol. 66, no. 12, pp. 6997–7009, Dec. 2018. DOI: 10.1109/TAP.2018.2874427

[8] G.-L. Huang, S.-G. Zhou, T.-H. Chio, C.-Y.-D. Sim, and T.-S. Yeo, "Wideband dual-polarized and dual-monopulse compact array for SAR system integration applications," *IEEE Geosci. Remote. Sens.*, vol. 13, no. 8, pp. 1203–1207, Aug. 2016. DOI: 10.1109/LGRS.2016.2576474

[9] J. Hirokawa, M. Ando, and N. Goto, "Waveguide-fed parallel plate slot array antenna," *IEEE Trans. Antennas Propag.*, vol. 40, no. 2, pp. 218–223, Feb. 1992. DOI: 10.1109/8.127406

[10] T. Wang, T. Tomura, J. Hirokawa, B. Pyne, P.R. Akbar, and H. Saito, "A feeding network with collinearly centered longitudinal coupling slots for a rectangular parallel-plate slot array antenna," *IEEE Trans. Antennas Propag.*, vol. 71, no. 7, pp. 5838–5849, July 2023. DOI: 10.1109/TAP.2023.3270458

[11] H. Xiong, J. Hirokawa, and T. Tomura, "A center-fed dual-polarized parallel-plate waveguide slot array antenna based on a feeding waveguide with centered longitudinal feeding slots," *IEEE Access*, vol. 11, pp. 93793–93803, 2023. DOI: 10.1109/ACCESS.2023.3310542